

# Slow magnetosonic waves generated in the plasmasphere by ionospheric terminator motion

A.S. Leonovich, D.A. Kozlov

Institute of Solar-Terrestrial Physics SB RAS, Irkutsk, 664033, Russia,

E mail leon@iszf.irk.ru

Accepted: 22 November 2011

---

**Abstract** A problem of the structure and spectrum of slow magnetosonic waves in a dipole plasmasphere is solved. The numerical solutions are found to the problem, for a distribution of the plasma parameters typical of the Earth's plasmasphere. The solutions allow us to treat the total electronic content oscillations registered above Japan as oscillations of one of the first harmonics of standing slow magnetosonic (SMS) waves. The results of numerical calculations of total electron content (TEC) oscillation amplitude are compared to the observations of the TEC oscillations and are shown to be in a good agreement with them.

© 2012 BBSCS RN SWS. All rights reserved

**Keywords:** MHD, slow magnetosonic waves, solar terminator, TEC oscillations

---

## Introduction

MHD waves are the lower-frequency part of electromagnetic oscillations of Earth's magnetosphere. There are two modes of MHD oscillations capable of propagating almost exactly along magnetic field lines – the Alfvén waves and slow magnetosonic (SMS) waves. Propagation of the fast magnetosonic (FMS) waves is not related to the magnetic field direction. Closed magnetic field lines cross the ionosphere in the Northern and Southern hemispheres. Because of the high conductivity, the ionosphere is almost ideally-reflecting boundary for the waves under consideration. Therefore the Alfvén and SMS oscillations can form standing (along the magnetic field lines) waves in the magnetosphere.

The structure and spectrum of standing Alfvén waves in dipole-like models of the magnetosphere was investigated by many authors [Radoski, 1967; Leonovich and Mazur, 1989; Chen and Cowley, 1989; Lee and Lysak, 1991; Wright, 1992 etc.]. Meanwhile, little attention to the standing SMS waves was paid [Taylor and Walker, 1987; Leonovich, Kozlov and Pilipenko, 2006; Klimushkin and Mager, 2008]. It is probably due to their rather large decrement, which makes eigen SMS-oscillations decay too fast to be registered. Nonetheless, they may well be observed in the magnetosphere when there is a strong enough source capable of generating such waves. Leonovich, Kozlov and Pilipenko (2006) study resonant SMS waves excited in the dipole magnetosphere by a monochromatic fast magnetosonic wave penetrating from the solar wind into the magnetosphere. The typical wavelength of such SMS oscillations both in the direction along magnetic field lines and in the azimuthal direction is of the order of the characteristic scale of magnetospheric plasma inhomogeneity. Across the magnetic shells, they have a typical resonance structure with a much smaller characteristic scale. Their amplitude decreases drastically along the magnetic field lines from the equatorial plane to the ionosphere. Therefore, such

oscillation is possible to register at high-orbit spacecraft only.

One of the possible application of theory of standing SMS oscillation appeared after the paper by Afraimovich et al. (2009) devoted to total electronic content (TEC) oscillations observed with GPS network in Japan. TEC oscillations in question are best registered at times close to the summer solstice. The oscillations appear in the ionospheric region over Japan 20-30 minutes after the evening solar terminator passes over the magnetoconjugated region of the Southern hemisphere. The terminator passes through the observation regions 1 hour later than the TEC oscillations start. Since the terminator at the midlatitudes moves at supersonic speed, the MHD oscillations cannot be related to the inner gravity waves generated by the terminator. These waves are most likely responsible for the oscillations of the total electronic content after the terminator passes over the observation point. The periods of the observed TEC oscillations were within the 15-30 minute range. Lower-frequency oscillations were filtered artificially to eliminate the effect of the GPS satellite movement. It was suggested that the magnetoconjugate regions of the ionosphere interact via Alfvén or SMS waves moving along the geomagnetic field lines. The specific periods of the first harmonics of standing Alfvén waves at the magnetic shells under study (~10 seconds) are very far from the periods of the observed TEC oscillations, so the generation of the observable MHD oscillations by the Alfvén wave appears to be ineffective. The periods of the first harmonics of standing SMS waves (~20 minutes) fit exactly in the required range. Afraimovich et al. (2009) conclude that the TEC oscillations related to the terminator transit in the magnetoconjugated region of the ionosphere are manifestation of one (or several) of the first harmonics of standing SMS waves.

This paper is aimed to confirm the hypothesis. We will calculate the total field of standing SMS waves in a dipole model of the Earth's plasmasphere and compare the results with the observational data. SMS

waves related to the terminator transit are likely to have a rather large typical wavelength across magnetic shells (comparable to the typical scale of magnetospheric inhomogeneity) while being fairly small-scale in the azimuthal direction.

This paper has the following structure. Section 2 deals with describing the model medium, deriving the basic equation for calculating the structure and spectrum of azimuthally small-scale standing SMS waves as well as obtaining analytical expressions for the oscillation field components. A numerical solution to the basic equation is found, the distributions of the oscillation field components along a magnetic field line are constructed and the results are discussed in Section 3. The Conclusion lists the main results of the paper.

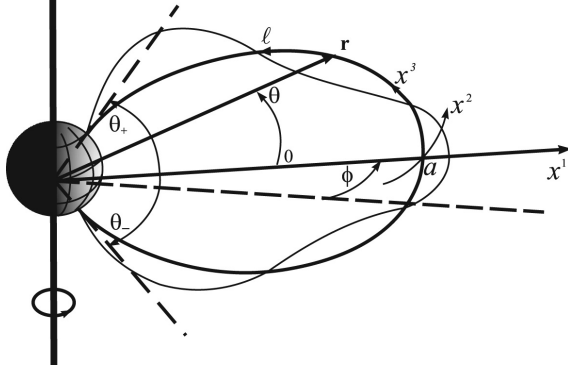


Fig. 1. The curvilinear orthogonal coordinate system  $(x^1, x^2, x^3)$  associated with magnetic field lines and the nonorthogonal coordinate system  $(a, \phi, \theta)$  used in numerical calculations. The structure of the 5th harmonic of standing SMS-waves along a magnetic field line is shown schematically.

## Model and governing equations

The model of plasmasphere with dipole-like magnetic field is shown on Figure 1. An orthogonal curvilinear coordinate system  $(x^1, x^2, x^3)$  related to the magnetic field lines geometry is used. The  $x^3$  coordinate is directed along the field line,  $x^1$  across the magnetic shells, and  $x^2$  in the azimuthal direction so that the coordinate system is right-handed. The element of length  $dl$  is defined by the relation

$$dl^2 = g_1(dx^1)^2 + g_2(dx^2)^2 + g_3(dx^3)^2, \text{ where}$$

$g_i (i=1,2,3)$  are the metric tensor components. We assume that the plasma and magnetic field are homogeneous with respect to the  $x^2$  coordinate. We will describe MHD oscillations using the set of equations for the ideal MHD:

$$\rho \frac{d\mathbf{v}}{dt} = -\nabla P + \frac{1}{4\pi} [\text{curl} \mathbf{B} \times \mathbf{B}], \quad (1.1)$$

$$\frac{\partial \mathbf{B}}{\partial t} = \text{curl}[\mathbf{v} \times \mathbf{B}], \quad (1.2)$$

$$\frac{\partial \rho}{\partial t} + \nabla(\rho \mathbf{v}) = 0, \quad (1.3)$$

$$\frac{d}{dt} \frac{P}{\rho^\gamma} = 0, \quad (1.4)$$

where  $\mathbf{B}$  and  $\mathbf{v}$  are the magnetic field intensity and plasma motion velocity vectors, respectively,  $\rho$  and  $P$  are the plasma density and pressure,  $\gamma$  is the adiabatic index. In the drift approximation the disturbed electric field  $\mathbf{E}$  is defined by  $\mathbf{E} = -[\mathbf{v} \times \mathbf{B}]/c$ .

The distribution of parameters of the unperturbed magnetosphere:  $\mathbf{B}_0, \mathbf{v}_0, \mathbf{E}_0, \rho_0, P_0$  is described by Eqs. 1.1-1.4 in steady state ( $\partial/\partial t = 0$ ). The plasma is assumed to be motionless ( $\mathbf{v}_0 = 0, \mathbf{E}_0 = 0$ ). Let us consider small perturbations  $\mathbf{B}', \mathbf{v}', \mathbf{E}', \rho', P'$  related to the MHD oscillations so that  $\mathbf{B} = \mathbf{B}_0 + \mathbf{B}'$ ,  $\mathbf{v} = \mathbf{v}'$ ,  $\mathbf{E} = \mathbf{E}'$ ,  $\rho = \rho_0 + \rho'$ ,  $P = P_0 + P'$ . We linearize the set of Eqs. 1.1-1.4 with respect to the disturbed field components. Each disturbed component can be presented as the sum of the Fourier harmonics of the form  $\exp(ik_2 x^2 - i\omega t)$ , where  $\omega$  is the oscillation frequency,  $k_2$  is the azimuthal wave number. From Eq. 1.1 we have

$$-i\omega \rho_0 v'_1 = -\nabla_1 P' + \frac{B_0}{4\pi \sqrt{g_3}} (\nabla_3 B'_1 - \nabla_1 B'_3), \quad (2.1)$$

$$-i\omega \rho_0 v'_2 = -ik_2 P' + \frac{B_0}{4\pi \sqrt{g_3}} (\nabla_3 B'_2 - ik_2 B'_3), \quad (2.2)$$

$$i\omega \rho_0 v'_3 = \nabla_3 P', \quad (2.3)$$

where  $v_i, B_i (i=1,2,3)$  are the covariant components of the disturbed velocity  $\mathbf{v}'$  and magnetic field  $\mathbf{B}'$ ,  $\nabla_i \equiv \partial/\partial x^i$ .

From Eqs. 1.3 and 1.4 we obtain

$$P' = -i \frac{\gamma}{\omega} \frac{P_0^{1-\sigma}}{\sqrt{g}} \left[ \nabla_1 \left( \frac{\sqrt{g}}{g_1} P_0^\sigma v_1 \right) + ik_2 \frac{\sqrt{g}}{g_1} P_0^\sigma v_2 + \nabla_3 \left( \frac{\sqrt{g}}{g_1} P_0^\sigma v_3 \right) \right],$$

where  $g = \sqrt{g_1 g_2 g_3}$ ,  $\sigma = 1/\gamma$ .

The disturbed electric field  $\mathbf{E}'$  can be represented via potentials  $\Phi$  and  $\Psi$

$$\mathbf{E}' = -\nabla_{\perp} \Phi + \nabla_{\perp} \times \Psi \frac{\mathbf{B}_0}{B_0}$$

where  $\nabla_{\perp} = (\nabla_1, \nabla_2, 0)$ . It is possible to express all the disturbed components of MHD oscillations through  $\Phi$  and  $\Psi$ :

$$\begin{aligned} v'_1 &= -\frac{cP^{-1}}{B_0} \left( ik_2 \Phi + \frac{g_2}{\sqrt{g}} \nabla_1 \Psi \right), \\ v'_2 &= \frac{cP}{B_0} \left( \nabla_1 \Phi - ik_2 \frac{g_2}{\sqrt{g}} \Psi \right), \\ v'_3 &= -i \frac{\nabla_3 P'}{\omega \rho_0}, \end{aligned} \quad (3)$$

$$\begin{aligned} B'_1 &= -i \frac{cg_1}{\omega \sqrt{g}} \nabla_3 \left( ik_2 \Phi + \frac{g_2}{\sqrt{g}} \nabla_1 \Psi \right), \\ B'_2 &= i \frac{cg_2}{\omega \sqrt{g}} \nabla_3 \left( \nabla_1 \Phi - ik_2 \frac{g_2}{\sqrt{g}} \Psi \right), \\ B'_3 &= i \frac{cg_3}{\omega \sqrt{g}} \left( \nabla_1 \frac{g_2}{\sqrt{g}} \nabla_1 \Psi - ik_2^2 \frac{g_1}{\sqrt{g}} \Psi \right) \end{aligned} \quad (3)$$

and to obtain an equation for disturbed pressure

$$\begin{aligned} \nabla_1 \hat{L}_T \nabla_1 \Phi - k_2^2 \left( \hat{L}_P \Phi + \frac{S^2}{A^2} \frac{\Phi}{\sqrt{g_1 g_2}} \nabla_1 \ln B_0 \nabla_1 \ln \frac{\sqrt{g_3} P_0^{\sigma}}{\rho_0} \right) = \\ = i \frac{k_2}{\omega} \left( \nabla_1 \hat{L}_T \frac{g_1}{\sqrt{g}} - \hat{L}_P \frac{g_2}{\sqrt{g}} \nabla_1 \right) \Psi, \end{aligned} \quad (4)$$

where

$$\begin{aligned} \hat{L}_T &= \frac{1}{\sqrt{g_3}} \nabla_3 \frac{p}{\sqrt{g_3}} \nabla_3 + p \frac{\omega^2}{A^2}, \\ \hat{L}_P &= \frac{1}{\sqrt{g_3}} \nabla_3 \frac{p^{-1}}{\sqrt{g_3}} \nabla_3 + p^{-1} \frac{\omega^2}{A^2} \end{aligned}$$

are the toroidal and poloidal longitudinal operators,

$S = \sqrt{\gamma P_0 / \rho_0}$  is the sound velocity in plasma,

$A = B_0 / \sqrt{4\pi \rho_0}$  is the Alfvén speed. By acting on

Eq. 2.2 with the operator  $\hat{L}_0$ , we obtain after some transformations

$$\begin{aligned} \frac{B_0 \sqrt{g_3}}{4\pi \rho_0} \hat{L}_0 \frac{B_0}{\sqrt{g_3}} \tilde{\Delta} \Psi + S^2 \bar{\Delta} \Psi + \omega^2 \Psi = \\ = -i \frac{B_0 \sqrt{g_3}}{4\pi k_2 \rho_0} \hat{L}_0 B_0 \hat{L}_T \nabla_1 \Phi - i \Phi k_2 S^2 \frac{g_3}{\sqrt{g}} \nabla_1 \ln \frac{\sqrt{g_3} P_0^{\sigma}}{B_0} \end{aligned} \quad (5)$$

where

$$\begin{aligned} \tilde{\Delta} &= \frac{g_3}{\sqrt{g}} \nabla_1 \frac{g_2}{\sqrt{g}} \nabla_1 - \frac{k_2^4}{g_2} + \nabla_3 \frac{g_2}{\sqrt{g}} \nabla_3 \frac{g_1}{\sqrt{g}}, \\ \bar{\Delta} &= \frac{B_0}{P_0^{\sigma}} \frac{1}{\sqrt{g_1 g_2}} \left( \nabla_1 \frac{p P_0^{\sigma}}{B_0} \nabla_1 - \frac{k_2^2}{p} \frac{P_0^{\sigma}}{B_0} + \right. \\ &\quad \left. + \nabla_3 \frac{\sqrt{g} P_0^{\sigma}}{g_3 \rho_0} \nabla_3 \frac{\rho_0}{B_0 \sqrt{g_3}} \right) \end{aligned}$$

are analogous to Laplace operator.

The right sides in Eqs. 4 and 5 tend to zero when we pass to homogeneous plasma. The functional in the left side of Eq. 4 yields a dispersion equation for the Alfvén waves  $\omega^2 = k_{\parallel}^2 A^2$ , where  $k_{\parallel}^2 \equiv k_3^2 / g_3$ , while the operator in the left side of Eq. 5 yields a dispersion equation for the magnetosonic waves:

$$\omega^4 - \omega^2 k^2 (A^2 + S^2) + k^2 k_{\parallel}^2 A^2 S^2 = 0, \quad (6)$$

where  $k^2 = k_{\perp}^2 + k_{\parallel}^2$ ,  $k_{\parallel}^2 = k_1^2 / g_1 + k_2^2 / g_2$ . Therefore, it is justified to conclude that the Alfvén oscillations are described by the scalar potential  $\Phi$ , and the magnetosonic waves by the longitudinal component of the vector potential  $\Psi$ . In an inhomogeneous plasma the right sides of Eqs. 4 and 5 describe coupling of these branches of MHD oscillations.

When  $S \ll A$ , or  $A \ll S$ , or  $|k_{\parallel}| \ll |k_{\perp}|$ , it is possible to get the approximate dispersion equations for fast magnetosonic (FMS) and slow magnetosonic (SMS) oscillations:

$$\omega^2 = k^2 C_F^2, \quad \omega^2 = k^2 C_S^2,$$

where  $C_F = (A^2 + S^2)^{1/2}$  and  $C_S = AS / (A^2 + S^2)^{1/2}$  are the phase speeds of the FMS and SMS waves, correspondingly.

The dispersion equation for SMS waves is similar to the dispersion equation for Alfvén waves. Both modes propagate along the magnetic field lines. The potential  $\Psi$  describes both the fast and the slow magnetosonic waves, and it is natural to represent it in the linear approximation as a sum  $\Psi = \Psi_F + \Psi_S$ , where the  $\Psi_F$  component refers to the FMS wave, and the  $\Psi_S$  component to the SMS wave.

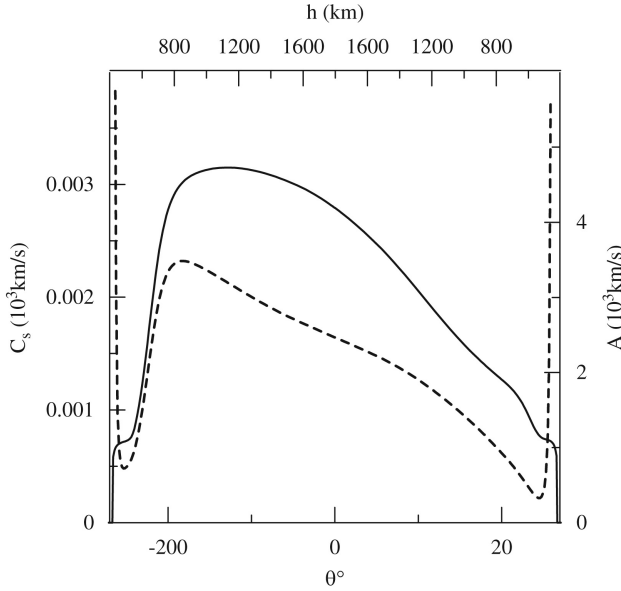


Fig. 2. Alfvén speed (dashed line) and SMS wave velocity distributions (solid line) along the field line crossing the Earth's ionosphere in the Northern hemisphere above Japan (37N, 138E) at 11h UT on June 14, 2008. The parameters of the medium were calculated using the numerical model of the plasmasphere by Krinberg and Tschilin (1984).

In order to calculate the distribution of parameters of background plasma along a magnetic field line in numerical calculations we use the numerical plasmasphere model by Krinberg and Tschilin (1984). Figure 2 shows distribution of Alfvén speed  $A$  and the

speed of SMS waves  $C_s$  along the magnetic field line crossing the Earth's ionosphere over Japan (37N, 138E) for June 14, 2008, at 11h UT. It is obvious that the inequality  $S \ll A$  is fulfilled along the entire field line. The parameters are calculated from the altitude of 80 km up to the field-line top. The strong asymmetry of the  $A$  and  $C_s$  profiles in the Northern and Southern hemisphere is due to the fact that the ionosphere in the Northern hemisphere is illuminated by the Sun, while being already in the shades in the Southern hemisphere.

The typical eigenfrequencies of the first harmonics of standing Alfvén and SMS waves differ by more than two orders of magnitudes in the magnetosphere model used. That means that coupling of the Alfvén and SMS waves on the closed field lines is negligible. For FMS waves with periods under study ( $> 10$  min), the entire magnetosphere is an opacity region. Therefore, in studying the structure of the SMS oscillations described by Eq. 5, we can assume that  $\varphi = 0$  in the right side and that the FMS waves from the solar wind do not penetrate into the plasmasphere, so  $\psi_F = 0$ . From Eq. 5 we obtain for SMS waves in the plasmasphere

$$\frac{B_0 \sqrt{g_3}}{4\pi\rho_0} \hat{L}_0 \frac{B_0}{\sqrt{g_3}} \tilde{\Delta} \psi_s + S^2 \bar{\Delta} \psi_s + \omega^2 \psi_s = 0. \quad (7)$$

The characteristic scales of first harmonics of standing SMS waves excited by the terminator transit over the ionosphere in the direction along magnetic field lines (along the  $x^3$  coordinate) and across magnetic shells (along the  $x^1$  coordinate) are much larger than their azimuthal scale (along the  $x^2$  coordinate) determined by the width of the terminator front. That allows us to employ the method of various scales for finding a solution to Eq. 7. To the main order, by retaining in Eq. 7 the terms proportional to the large azimuthal wave number  $k_2$  (determined as the value inverse to the azimuthal wavelength), we get

$$\frac{\sqrt{g_3} \rho_0}{\sqrt{g} B_0 P_0^\sigma} \nabla_3 \frac{\sqrt{g} P_0^\sigma}{g_3 \rho_0} \nabla_3 \frac{B_0}{g_2 \sqrt{g_3}} \psi_s + \frac{\omega^2}{g_2 C_s^2} \psi_s = 0 \quad (8)$$

The solution to this equation may be sought in the form  $\psi_s = V(x^1) S(x^1, x^3)$ , where the function  $V(x^1)$  is determined by the source of oscillations under study and describes their structure across the magnetic shells. The function  $S(x^1, x^3)$  describes the longitudinal structure of  $\psi_s$  and is defined by Eq. 8. It is convenient to introduce the function  $H(x^1, x^3) = S(x^1, x^3) B_0 / (g_2 \sqrt{g_3})$  that is described by the equation

$$\frac{\partial}{\partial \ell} \alpha(x^1, x^3) \frac{\partial H}{\partial \ell} + \frac{\omega^2}{C_s^2} \alpha(x^1, x^3) H = 0,$$

where  $\partial / \partial \ell = (\sqrt{g_3})^{-1} \partial / \partial x^3$ ,  $\alpha = P_0^\sigma \sqrt{g_1 g_2} / \rho_0$ .

Using Eqs. 3, we can express the main oscillation component via  $\psi_s$ . To find longitudinal component of plasma oscillation velocity, it is possible to use the fact that total pressure in the SMS wave is practically not disturbed, that is  $P' + B_0 B'_\parallel / 4\pi = 0$ . It yields

$$v_\parallel \equiv v_3 / \sqrt{g_3} \approx V(x^1) \frac{ck_2^2}{4\pi\rho_0 \omega^2} \frac{\partial H(x^1, x^3)}{\partial \ell}.$$

As our numerical calculations showed, the oscillations of plasma concentration near the ionosphere determining the TEC oscillations are mainly linked to the longitudinal velocity. Keeping only the main terms  $\sim v_\parallel$  in the linearized Eq. 1.3, we

obtain the following expression for the disturbed density

$$\rho' \approx i \frac{v_{\parallel}}{\omega \sqrt{g_1 g_2}} \frac{\partial}{\partial \ell} \rho_0 \sqrt{g_1 g_2}$$

which serves as a basis for determining the plasma concentration oscillations.

### Numerical calculation results and discussion

Our calculations refer to June 14, 2008, which is discussed by Afraimovich et al. (2009), when the TEC oscillations related to the terminator transit over the magnetoconjugate ionosphere were observed on the territory of Japan. The field line crossing the Northern hemisphere at the point with coordinates (37N, 138E) is taken as an example.

In the numerical calculations the coordinate system  $(a, \Phi, \theta)$  related to the field line of a dipole magnetic field was used (see Figure 1), where  $a$  is the equatorial radius of a field line,  $\Phi$  is the azimuthal angle,  $\theta$  is the latitude measured from the equator. The field line equation in this coordinate system is

$$r = a \cos^2 \theta$$

and the length element

$$d\ell = a \cos \theta (1 + 3 \sin^2 \theta)^{1/2} d\theta$$

The dipole magnetic field intensity is determined

$$\text{by } B_0(a, \theta) = \bar{B}_0 (a_0 / a)^3 (1 + 3 \sin^2 \theta)^{1/2} \cos^{-6} \theta,$$

where  $\bar{B}_0 = 0.32 \text{ Gauss}$  is magnetic field magnitude on the field line with equatorial radius  $a_0 = R_E$ ,  $R_E$  is the Earth's radius. The metric tensor components are

$$g_1 = \cos^6 \theta / (1 + 3 \sin^2 \theta), \quad g_2 = a^2 \cos^6 \theta$$

Figure 3 presents the diurnal variation of the periods of the first 6 harmonics of standing SMS waves on the field line mentioned above. One's attention is drawn to the fact that the oscillation period of the first harmonic ( $\sim 300$ - $400$  minutes) is very different from those of all the other harmonics (less than 90 minutes). As was expected, the difference between the oscillation periods calculated both numerically and in the WKB approximation decreases with the harmonic number  $n$ . The range of the TEC oscillation periods observed by Afraimovich et al. (2009) includes harmonics with  $n = 4, 5, 6$ . Given the fact that oscillations with periods larger than 30 minutes were filtered in the observations, one can expect lower-frequency harmonics to be present as well. However they are difficult to extract against the background of dynamical effects related to the motion of the GPS satellites.

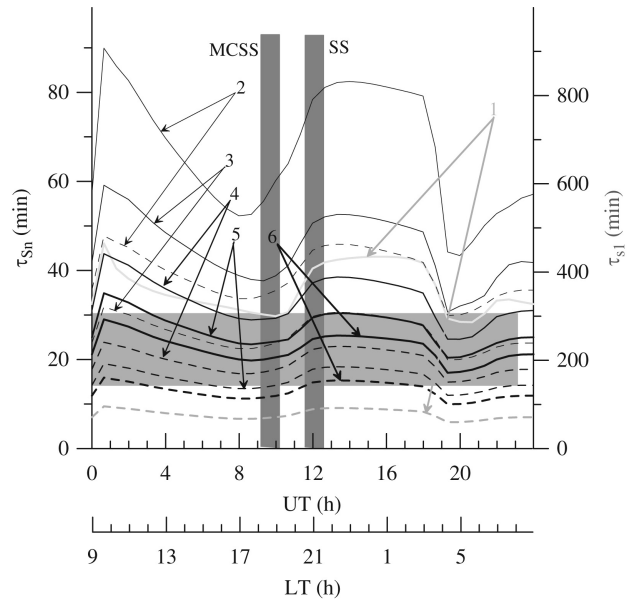


Fig. 3. Diurnal variation of the oscillation periods of the first 6 harmonics of standing SMS waves on June 14, 2008 for the field line crossing the ionosphere at (37N, 138E). The dashed lines denote the oscillation periods in the WKB approximation, the solid lines show the periods from the numerical solution. The oscillation period of the first harmonic  $\tau_{s1}$  is shown in grey (vertical axis to the right). The horizontal grey band is the range of the periods of the TEC oscillations observed by Afraimovich et al. (2009). The vertical grey bands are the characteristic times of the terminator transit at the observing point (SS) and at the magnetoconjugate point (MCSS).

In order to find the standing SMS wave amplitude distribution we need to specify the amplitude of a component of the waves at any point on the field line. Though there are no direct measuring of such oscillations simultaneously with observations of the TEC oscillations in the magnetoconjugate ionosphere, Onishi et al. (2009) provide data on simultaneous observations of the TEC oscillations and the longitudinal velocity component of the plasma

oscillations  $v_{\parallel}$  by the DEMETER satellite, flying over the region of the TEC oscillations at altitudes of 650-700 km. During several passages over North America,

the DEMETER satellite registered  $v_{\parallel}$  oscillations with amplitudes 20-80 km/s and the accompanying TEC oscillations with amplitudes  $(0.1 - 0.6) \cdot 10^{16} \text{ m}^{-2}$ .

We will set the oscillation amplitude  $|v_{\parallel}| = 50 \text{ km/s}$  at altitude 650 km in our subsequent calculations. Let us assume that the spectrum of the observed oscillations is dominated by oscillations of a certain harmonic, so

that the set amplitude of  $v_{\parallel}$  determines the oscillations of this particular harmonic.

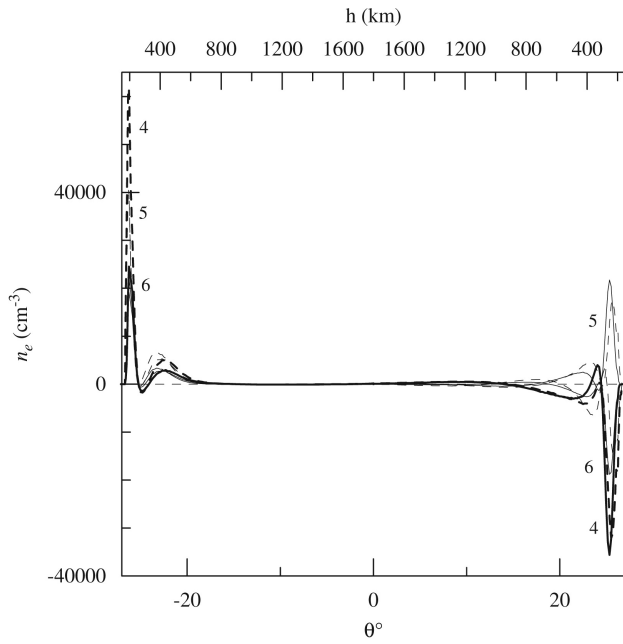


Fig. 4. Distribution of the electron concentration  $n_e$  oscillations for the 4th, 5th, 6th harmonics of standing SMS waves along the field line crossing the ionosphere at (37N, 138E) at 11h UT on June 14, 2008. The dashed curves present the distribution of  $n_e$  in the WKB approximation, the solid lines show  $n_e$  obtained numerically.

Figure 4 presents the distribution of  $n_e$  along the field line for the 4, 5 and 6th harmonics of standing SMS waves. Electron concentration  $n_e$  exhibits sharp peaks at altitudes  $\sim 200$  km in the Southern hemisphere and at  $\sim 300$  km in the Northern hemisphere. This fact enables us to estimate the magnitude of the TEC oscillations by integrating  $n_e$  along a magnetic field line. Due to a sharp peak in the  $n_e$  distribution, the magnitude of

$$N_{\text{ell}} = \int_{\ell_{\pm}}^{\ell} n_e d\ell$$

at altitudes  $h > 400$  km should not be much different from the TEC oscillation amplitudes obtained by integrating along the line drawn from the GPS receiver on the Earth's surface to the satellite. Here the " $\pm$ " refers to the upper boundary of the ionospheric conductive layer in the Northern and Southern hemispheres, respectively, and integration is along the magnetic field line.

Figure 5 presents the distribution of  $N_{\text{ell}}$  in the Southern and Northern parts of the plasmasphere for the 4th, 5th, 6th harmonics of standing SMS waves. It is evident that the thus-obtained oscillation amplitudes  $|N_{\text{ell}}| \sim (0.4 - 0.8) \cdot 10^{16} \text{ m}^{-2}$  for  $h > 400$  km, tally well

with the TEC oscillation amplitudes observed by Onishi et al. (2009). It is possible that Onishi et al. could also observe standing SMS oscillations. TEC oscillation amplitudes observed by Afraimovich et al. (2009) are 10 times as small  $(0.01 - 0.04) \cdot 10^{16} \text{ m}^{-2}$ . Figure 6 shows the spatio-temporal distribution of  $N_{\text{ell}}$  in the Southern and Northern for the 4th harmonic of standing SMS waves.

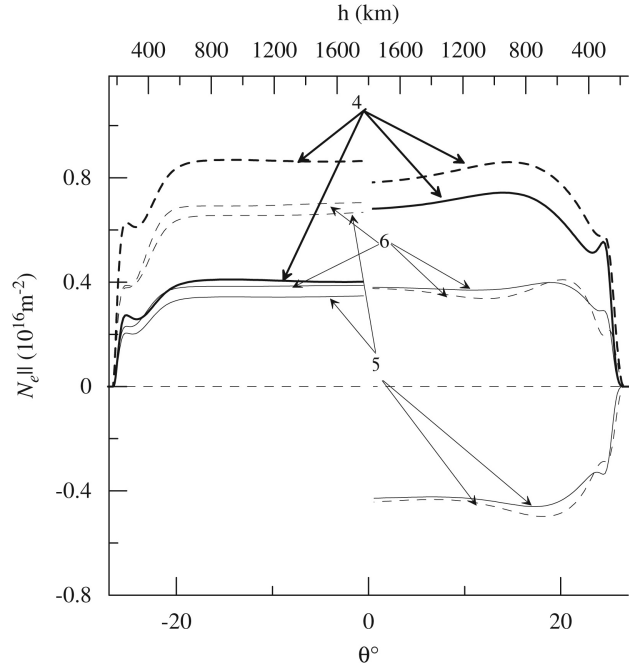


Fig. 5. Distribution of the total electronic content  $N_{\text{ell}}$  for the 4th, 5th, 6th harmonics of standing SMS waves along the field line crossing the ionosphere at (37N, 138E) at 11h UT on June 14, 2008. The dashed curves present the distribution of  $N_{\text{ell}}$  in the WKB approximation, the solid lines show  $N_{\text{ell}}$  obtained numerically.

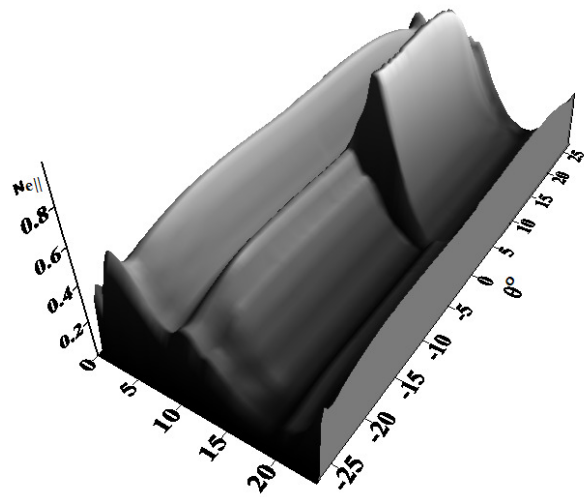


Fig. 6. Spatio-temporal distribution of the total electronic content  $N_{\text{ell}}$  for the 4th harmonics of standing SMS waves

along the field line crossing the ionosphere at (37N, 138E) on June 14, 2008.

## Conclusion

Let us list the main results of this study.

1. Equation 8 is obtained for calculating the field structure of azimuthally small-scale standing SMS waves in a dipole-like plasmasphere. The numerical solutions are obtained to this equation for the plasma parameters distributed similarly to the Earth's plasmasphere.
2. The spectrum of the oscillation periods of the first harmonics of standing SMS waves is calculated on the field line crossing the Earth's ionosphere at (37N, 138E) at 11h UT on June 14, 2008. Of the harmonics we have calculated, the 4th, 5th and 6th harmonics fall within the range of periods of the observed oscillations treated by Afraimovich et al. (2009) as standing SMS waves.
3. Calibration of the amplitudes of the above field components in the numerical calculations relied on the data of simultaneous observations of the TEC oscillations and the  $V_{||}$  oscillations by the DEMETER satellite in. The TEC oscillations  $|N_{\text{osc}}| \sim (0.4-0.8) \cdot 10^{16} \text{ m}^{-2}$  calculated by us for the 4th, 5th, 6th harmonics of standing SMS waves are in good agreement with TEC oscillations observed by Onishi et al. (2009).

## Acknowledgements

The authors are grateful to A.V. Tashchilin and L.A. Leonovich for computing the background plasma parameters that we used in our numerical calculations. This work was partially supported by RFBR grant №09-02-00082 and №10-05-00113 and by Program of presidium of Russian Academy of Sciences №4 and OFN RAS №15.

## References

- Afraimovich, E. L., Edemskiy, I. K., Leonovich, A. S., Leonovich, L. A., Voeykov, S. V., and Yasyukevich, Y. V.: 2009, *Geophys. Res. Lett.* 36, L15106, doi:10.1029/2009GL039803.
- Chen, L., and Cowley, S. C.: 1989, *Geophys. Res. Lett.* 16, 895.
- Klimushkin, D. Yu., Mager, P. N.: 2008, *Planet. Space Sci.* 56, 1273.
- Krinberg, I. A., Tashchilin, A. V.: 1984, *Ionosphere and Plasmosphere*, (in Russian), Nauka, Moscow.
- Lee, D.-H., and Lysak, R. L.: 1991, *J. Geophys. Res.* 96, 5811.
- Leonovich, A. S., and Mazur, V. A.: 1989, *Planet. Space Sci.* 37, 1095.
- Leonovich, A. S., and Kozlov, D. A.: 2009, *Plasma Phys. Control. Fus.*, 51, 085007, doi:10.1088/0741-3335/51/8/085007
- Leonovich, A. S., Kozlov, D. A., Pilipenko, V. A.: 2006, *Ann. Geophys.* 24, 2277.
- Onishi, T., Tsugawa, T., Otsuka, Y., Berthelier, J.-J., Lebreton, J.-P.: 2009, *Geophys. Res. Lett.* 36, L11808, doi:10.1029/2009GL038156.
- Radoski, H. R.: 1967, *J. Geophys. Res.* 72, 4026.
- Taylor, J. P. H., Walker, A. D. M.: 1987, *J. Geophys. Res.* 92, 10046.
- Wright, A. N.: 1992, *J. Geophys. Res.* 97, 6429.